ADVANCED ENERGY MATERIALS
www.advenergymat.de

Triperylene Hexaimides Based All-Small-Molecule Solar Cells with an Efficiency over 6% and Open Circuit Voltage of 1.04 V

Ningning Liang, Dong Meng, Zetong Ma, Bin Kan, Xiangyi Meng, Zhong Zheng, Wei Jiang, Yan Li, Xiangjian Wan, Jianhui Hou, Wei Ma,* Yongsheng Chen,* and Zhaohui Wang**

Bulk-heterojunction (BHJ) organic solar cells (OSCs) comprising of an electron donor (*p*-type) and an acceptor material (*n*-type), have attracted extensive interests for researchers due to these attractive advantages, including low cost, solution processability, lightweight, flexibility, and the possibility of large-scale production.[1–3] The performance of OSCs depends highly on the energy levels, the absorption ability, and the charge transfer mobility of the donor and acceptor materials. Thus, much efforts have been devoted to the design and synthesis of novel donors and acceptors. Among them, the donor materials can be divided into polymeric donor (P_D), small molecular donor (M_D), and the acceptors also can be divided into fullerene molecular acceptors (F-M_A), non-fullerene small molecular acceptor (NF-M_A), and polymeric acceptors (P_A).

According to the classification of the donors and acceptors, the OSCs can be separated into six types: P_D/F-M_A,[4–8] P_D/NF-M_A,[9–31] P_D/P_A ("all-polymer"),[32–36] M_D/F-M_A ("all small molecule"),[37–39] M_D/P_A,[39] and M_D/NF-M_A ("non-fullerene all small molecule", NF-ASM).[40–42] Due to the intense investigations on the design and synthesis of donors and acceptors with new chemical structures, as well as the optimization of the BHJ morphology and device architecture and so on, the power conversion efficiencies (PCEs) of the single heterojunction OSCs based on P_D/F-M_A, P_D/NF-M_A, and M_D/F-M_A have exceeded to 10.5%,[43–46] 12.00%,[47] and 10.00%,[48] respectively. The all-polymer (P_D/P_A) OSCs also have achieved great successes with the highest PCE of 8.27%.[49] Compared with those types, the latter two small molecular donor based (M_D/P_A and M_D/NF-M_A) OSCs have relatively lower PCEs with 4.82%[50] and 5.44%[51], respectively. It is interesting to note that all-small-molecular OSCs based on perylene diimide (PDI) were relatively rarely studied and PCEs over 3% have rarely been reported.[40,52–55]

However, small molecules offer several advantages such as better-defined structure, less batch-to-batch variation, fine-tunable energy level and absorption, and deep-understanding the relationship between chemical structure and device performance in comparison with polymer materials.[56] Thus, small molecules as an interesting and developing sub-branch in OSCs field are promising. What's more, the non-fullerene small molecular acceptors, namely, NF-M_A have attracted broad interests of researchers from home and abroad owing to the strong absorption ability in visible light region, good electron-accepting ability, higher electron mobility, and the ability of fine-tuning electronic energy levels via chemical modification.[47,57–60] As one of the typical electronic acceptor, PDI derivatives have been paid great attention and have achieved fast advances during the past few years. Importantly, the PCEs of PDI-based PSCs have exceeded 9% that could be comparable with the fullerene-based polymer solar cells (PSCs),[61,62] due to chemical functionalization in the bay, non-bay position, or imide group as well as the optimization of device architecture and donor materials.[63–67] In addition, in recent years, the three-dimensional (3D) PDI small molecule acceptors have got great achievements with the advantages of high extinction coefficient, favorable BHJ morphology featuring a small domain size, and a higher open circuit voltage (V_{oc}).[68–71]

In addition, for OSCs, one of the most important factors that limits the efficiency is the significant loss in energy (E_{loss}) from the band gap (E_g) and the V_{oc} of the device, compared to the other types of solution-processed thin film solar cells, such as perovskite solar cells.[72,73] In practice, it is well known that the E_{loss} is typically 0.7–1.0 eV in efficient OSCs evaluated by comparing the optical band gap (E_g^{opt}) with V_{oc}, while it is less than 0.5 eV for perovskite solar cells.[74–76] The E_{loss} in solar cells is attributed to three factors, including the radiative recombination originating from the absorption above the band gap, the

N. Liang, D. Meng, Z. Ma, Z. Zheng, W. Jiang, Y. Li, Prof. J. Hou, Prof. Z. Wang
Institute of Chemistry
Chinese Academy of Sciences
Beijing 100190, China
E-mail: hjhzlz@iccas.ac.cn; wangzhaohui@iccas.ac.cn
N. Liang, D. Meng, Z. Ma, Z. Zheng
University of Chinese Academy of Sciences
Beijing 100049, China
B. Kan, X. Wan, Prof. Y. Chen
Key Laboratory of Functional Polymer Materials
Center for Nanoscale Science and Technology
Institute of Polymer Chemistry
College of Chemistry
Collaborative Innovation Center of Chemical Science and Engineering (Tianjin)
Nankai University
Tianjin 300071, China
E-mail: yschen99@nankai.edu.cn
X. Meng, Prof. W. Ma
State Key Laboratory for Mechanical Behavior of Materials
Xi'an Jiaotong University
Xi'an 710049, China
E-mail: msewma@mail.xjtu.edu.cn

DOI: 10.1002/aenm.201601664

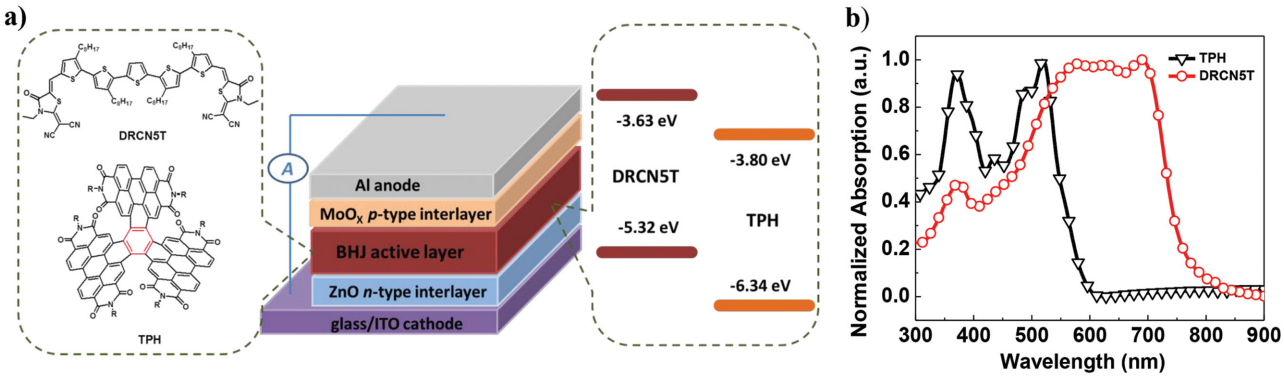

Figure 1. a) Device structure, molecular structure, and energy level diagram of the donor DRCN5T and acceptor TPH. b) Normalized UV–vis absorption spectra of pure donor and pure acceptor films.

additional radiative recombination from the absorption below the band gap, and the non-radiative recombination.[61] Therefore, it is essential to design and explore the OSCs with relatively low E_{loss} and high V_{oc} as well as keeping a high quantum efficiency for charge generation, to further enhance the PCE of OSCs.[72]

Herein, we adopted a small molecular material DRCN5T as the donor with the optical band gap of 1.60 eV[48] and a 3D-PDI acceptor that consists of three PDI subunits adjoining one single benzene ring to study the effect of thermal annealing (TA) treatment on the crystalline and orientation of donor and acceptor molecules and thereby the performance of NF-ASM OSCs. Upon TA treatment, the PCE of the BHJ devices was enhanced from 0.47% to 6.16%. To our best of knowledge, the PCE is among the highest values as reported in NF-ASM OSCs. In addition, the energy loss (E_{loss}) calculated from the difference between the optical band gap of DRCN5T and the eV_{oc} is as low as 0.56 eV.

As displayed in **Figure 1**, the conjugated 3D PDI-based acceptor consists of three PDI subunits, and each PDI subunit is linked into one benzene ring via double carbon–carbon bonds, namely, triperylene hexaimides (TPH). UV–vis absorption spectrum of TPH film has a strong and broad absorption at the region of 300–600 nm, complementary to that of the DRCN5T film from 500 to 780 nm, which is beneficial to utilize the visible region of the sunlight. The absorption edge of DRCN5T at 777 nm corresponds to an optical band gap of 1.60 eV, consistent with the previous literature.[48] Meanwhile, cyclic voltammetry (CV) measurements were carried out in acetonitrile/0.1 M tetrabutylammonium hexafluorophosphate (Bu_4NBF_4) solution. From Figure S1 (Supporting Information), the highest occupied molecular orbital (HOMO) and lowest unoccupied molecular orbital (LUMO) of DRCN5T film calculated from the onset oxidation and reduction potentials were estimated to be –5.32 and –3.63 eV, respectively; the HOMO and LUMO of TPH film were –3.80 and –6.34 eV, assuming that the Fc/Fc^+ had an absolute energy level of –4.80 eV to vacuum. Thus, the band gap measured via CV method (E_g^{cv}) is 1.69 eV.

In order to explore the photoelectronic property of TPH in NF-ASM OSCs, photovoltaic devices were prepared with an inverted device structure of ITO/ZnO/DRCN5T:TPH/MoO_x/Al, as shown in Figure 1a. Chloroform (CF) was used as the solvent, and the films were optimized by carefully controlling the weight ratio of donor and acceptor, the thermal temperature from room temperature to 190 °C, and the thermal time. The thickness of all BHJ layer was controlled to about 110 nm. The photovoltaic parameters of DRCN5T:TPH devices as-cast and with TA-treatment (100 °C) at different donor/acceptor ratio were summarized in Table S1 (Supporting Information) and the corresponding current–density/voltage (*J*–*V*) curves and the external quantum efficiency (EQE) spectra were shown in Figure S2 (Supporting Information). As shown, the device parameters of DRCN5T:TPH BHJ layers as-cast showed a poor short-circuit current density (J_{sc}) and fill factor (FF); fortunately, the DRCN5T:TPH BHJ layers after TA (100 °C) treatment exhibited a significant enhancement, especially the J_{sc} and FF, making the PCE improved from 0.47% to 5.37%. Then the thermal temperature and the thermal time were optimized carefully as shown in Tables S2 and S3 (Supporting Information). The optimal condition for DRCN5T:TPH BHJ layers was under 160 °C thermal treatment for 20 min. Under this condition, the DRCN5T:TPH devices showed a PCE_{max} of 6.16% with a J_{sc} of 11.59 mA cm^{-2}, a V_{oc} of 1.04 V, improving by 12 times. Those data were summarized in **Table 1** and the corresponding *J*-*V* curves and EQE spectra were shown in **Figure 2**.

In addition, the energy loss ($E_{loss}^{opt} = E_g^{opt} - eV_{OC}$) is only 0.56 eV, if the band gap is the optical band gap (E_g^{opt}), which is among the lowest E_{loss} in organic solar cells.[72–74] If the band gap is E_g^{CV} measured by CV method, the E_{loss}^{CV} is about 0.65 eV. According to the literature, we also used another method to evaluate the band gap based on the crossing point between the absorption and emission spectra.[61] As shown in Figure S4a and Table S4 (Supporting Information), the band gap is about 1.68 eV, and

Table 1. Photovoltaic parameters of the solar cells based on DRCN5T:TPH as-cast and TA treatment at different conditions under AM 1.5G illumination of 100 mW cm^{-2}.

Blend		V_{oc} [V]	J_{sc} [mA cm^{-2}]	FF	PCE [%]
DRCN5T:TPH	As-cast	1.06	1.61	0.28	0.47
	100 °C for 10 min	1.05	11.05	0.47	5.37
	160 °C for 10 min	1.04	11.52	0.50	5.78
	160 °C for 20 min	1.04	11.59	0.51	6.16

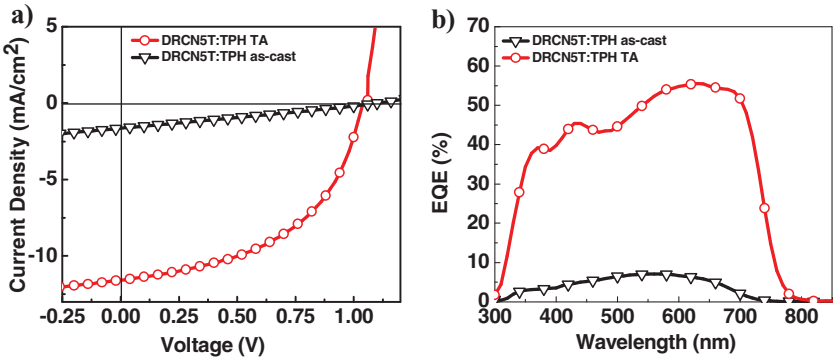

Figure 2. a) *J–V* curves and b) EQE spectra of solar cell devices as-cast and with TA treatment (160 °C) at the optimal donor/acceptor ratio.

the E_{loss} is about 0.64 eV. To the best of our knowledge, the V_{oc} of 1.04 V is among the highest value in this system with E_g of about 1.60 eV.[5,7,10,17,18,48]

As shown from the photoluminescence (PL) spectra in Figure S4b (Supporting Information), the fluorescence of acceptor TPH was completely quenched by the donor DRCN5T in blend film, indicating that the charge separation can occur efficiently at the surface of donor and acceptor. In addition, the morphology of DRCN5T:TPH blend films as-cast and with TA treatment were characterized by atomic force microscopy (AFM), resonant soft X-ray scattering (RSoXS), and grazing incidence wide-angle X-ray scatterings (GIWAXS). First, the surface morphology of the BHJ active layers was studied by tapping model AFM. The height images in **Figure 3**a,b showed that there were significant differences between the morphology of DRCN5T:TPH blend film as-cast and that of the TA-treatment blend film. The DRCN5T:TPH blend film as-cast had relatively smoother and more uniformed surfaces with the root-mean-square (RMS) roughness of 0.43 nm. Thus, there were no phase separation to form pathways for holes and electrons transporting. Upon TA treatment, the BHJ active layer had a significant phase separation, larger domain size, and rougher surfaces with RMS up to 1.47 nm. Benefiting from the TA treatment, the BHJ active layer had favorable morphology with optimal domain size and favorable transport pathway, which was good for the charge separation and transport.

RSoXS was performed to investigate the spatial dimensions of phase separation at different length scales and the relative domain purity.[77] A photon energy 284.2 eV was utilized to provide high small molecular donor/acceptor contrast between blend active layer with and without TA treatment. As shown in Figure 3c, the DRCN5T:TPH active layer as-cast presented low scattering intensity and thus weak phase separation; but after TA treatment, the active layer had a higher scattering intensity and multiple scattering peaks. According to the domain spacing revealed at the $\xi = 2\pi/q$ (ξ is the corresponding mode phase distribution in real space), the DRCN5T:TPH active layer as-cast had a small and broad characteristic mode length scale with $\xi \approx 41$ nm, whereas for TA-treatment blend, the dominant scattering peak reveals a lager length scale with $\xi \approx 51$ nm. The total scattering intensity (TSI) data can be acquired by integrating the scattering profiles and further to extract the relative domain purity. As shown in Figure 3c, the relative domain purity in DRCN5T:TPH active layer with TA treatment and DRCN5T:TPH blend as-cast was 1.00 and 0.76, respectively. The impure and relative small domains of the DRCN5T:TPH blend as-cast were negative to the charge transport and led to a high bimolecular recombination and low FF. Thus, along with the TA treatment, the slightly large and pure domains balanced the exciton dissociation and charge transport, corresponding to the high J_{sc} and FF.

These above phenomena can also be observed from the absorption spectra of pure DRCN5T, blend films as-cast and with TA treatment as shown in Figure 3d. The absorption ability of blend film was enhanced significantly after TA treatment, while it was quite weak for as-cast blend in around about 550–750 nm; but it was still lower than that of the pure DRCN5T film. Thus, the introduction of acceptor TPH would weaken the π–π stacking of donor DRCN5T. Therefore, GIWAXS were characterized to investigate the effect of TA treatment on the crystallinity, molecular packing, and orientation in pure and blend films.[78] **Figure 4**a,b showed that TPH acceptor film exhibited amorphous state, even with TA treatment. For pure

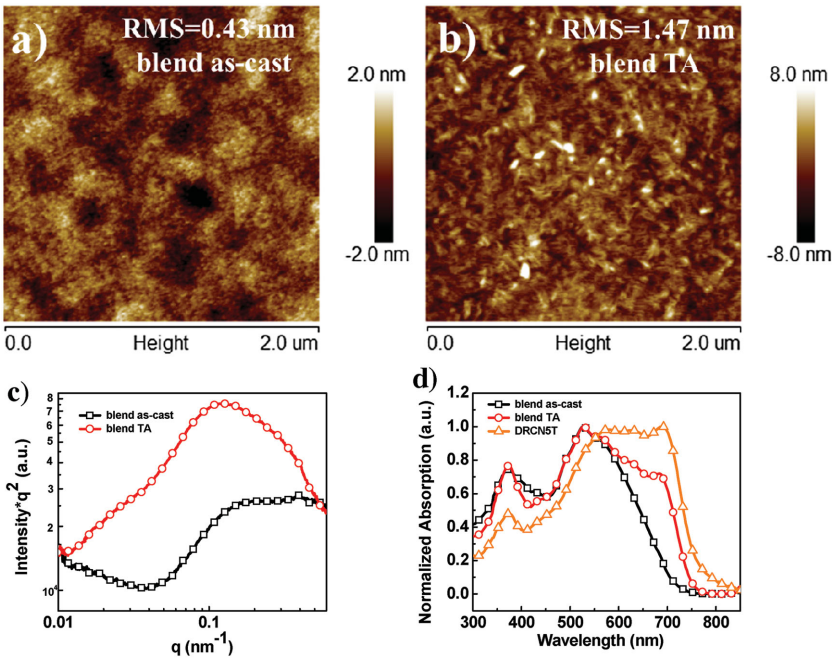

Figure 3. a,b) Tapping mode AFM height of DRCN5T:TPH as-cast and with TA treatment. c) RS_OXS profiles of blend films as-cast and with TA treatment, d) absorption spectra of DRCN5T, blend films as-cast and with TA treatment.

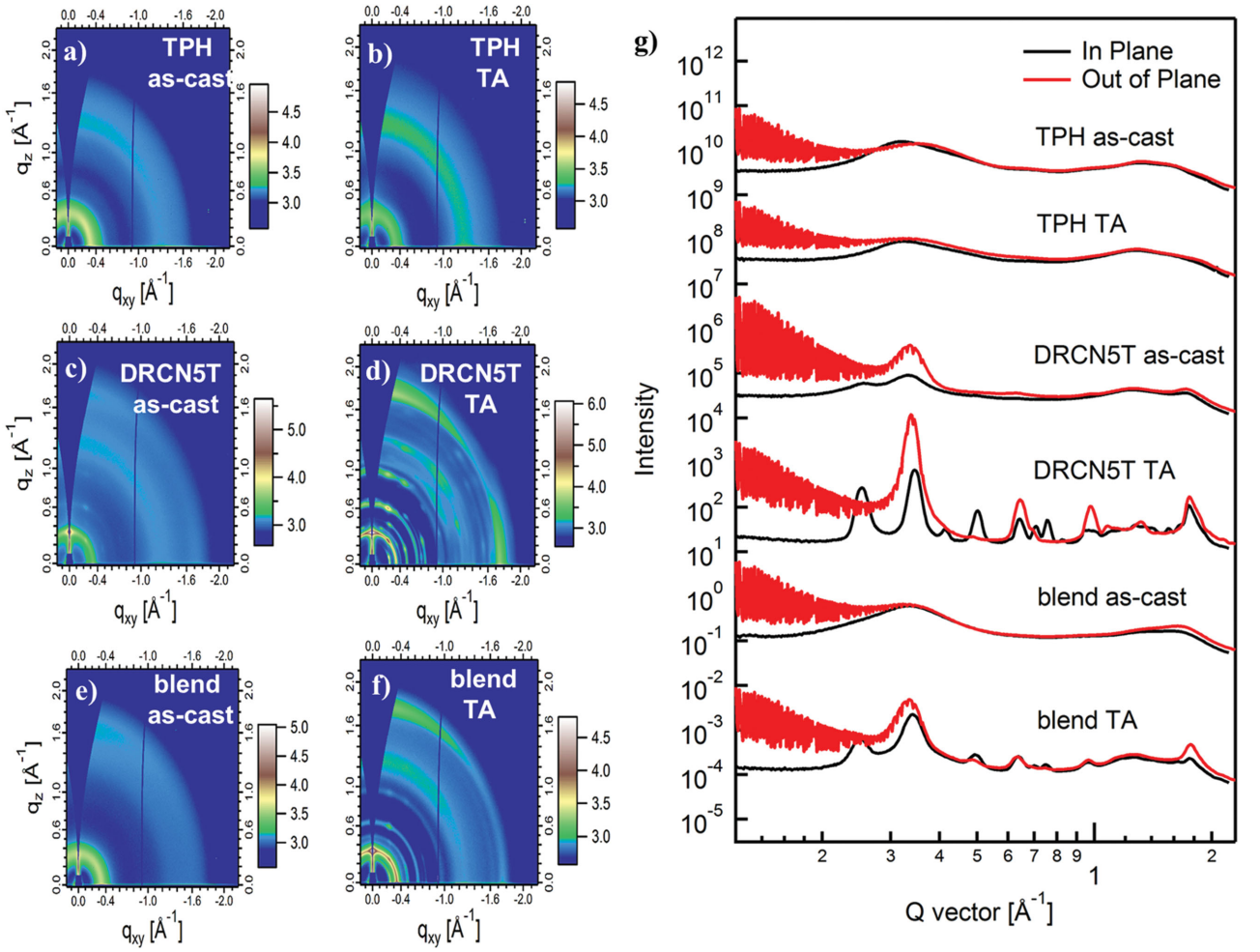

Figure 4. a–f) 2D GIWAXS patterns and g) scattering profiles of out-of-plane and in-plane for the acceptor TPH, donor DRCN5T, and blend active layers as-cast and with TA treatment.

DRCN5T donor, the film as-cast took on a weak crystallinity and showed unclearly lamellar (100) scattering peak (q = 0.33 Å^{-1}) and π–π (010) scattering peak (q = 1.72 Å^{-1}), corresponding to an inter-chain distance and π–π stacking distance of 19 and 3.65 Å, respectively. But the crystallinity and π–π stacking of pure DRCN5T film after TA treatment were significantly enhanced and showed pronounced lamellar (h00) peaks and strong (010) peak (q = 1.75 Å^{-1}, d = 3.59 Å) in the in-plane and out-of-plane directions. The DRCN5T:TPH blend film as-cast exhibited almost no diffraction peak, indicating the amorphous state of the DRCN5T and TPH. After processing with TA treatment, the blend films showed obvious diffraction peaks, but the crystallinity and π–π stacking of DRCN5T molecules were weakened in comparison with the pure film, especially in the in-plane direction for π–π stacking peak. This indicates that the DRCN5T has a dominant face-on orientation when blended with the TPH, which is beneficial to charge transport in the vertical direction and results in a high FF. Compared to the as-cast blend film, the enhancement ordering for DRCN5T molecules in TA-treatment blend is in favor for improving the hole mobility. These results revealed that while the introduction of acceptor weakened the crystallinity of DRCN5T in the in-plane and out-of-plane directions as well as weakened the π–π stacking in the in-plane direction, the crystallization of the donor DRCN5T in the TA blend film leads to the appropriate phase separation and purer domains, which results in both increased J_{sc} and FF.

The hole (μ_h) and electron (μ_e) mobilities were further evaluated by the space-charge-limited current (SCLC) method with the device structure of ITO/PEDOT:PSS/DRCN5T:TPH/Au and ITO/ZnO/DRCN5T:TPH/Al, respectively, to probe the effect of TA treatment on the charge transporting behavior of DRCN5T, TPH and blend active layers. Those results were presented in Table S5 and Figure S6 (Supporting Information). As shown, the mobilities of DRCN5T and the BHJ active layers were enhanced significantly after TA treatment due to the closer lamellar packing and π–π stacking enhancement by TA treatment. In addition, the μ_h of active layers were higher than μ_e, indicating that the relative lower μ_e limits the enhancement of J_{sc} and FF. Thus, it is a challenge for 3D-PDI based derives to enhance the electron mobility for higher J_{sc} and FF, on the basis of maintaining the favorable film morphology. According to the SCLC mobility, the μ_e of TPH pure film was enhanced when the donor DRCN5T was added, demonstrating that the

donor material DRCN5T maybe a bipolar compound. Therefore, the field-dependence of the carrier mobilities was performed and found that the DRCN5T molecules exhibited a high μ_h of 0.017 $cm^2\ v^{-1}\ s^{-1}$ as well as μ_e of 0.0031 $cm^2\ v^{-1}\ s^{-1}$. The ambipolar charge transport characteristics for donor DRCN5T are contributed to the charge carrier balance in the BHJ active layer, as shown in Figure S7 (Supporting Information).

In addition, we also used the analogue of TPH, namely, STPH consisting of three PDI subunits with each PDI subunit linked into one benzene ring via single carbon–carbon bond, as shown in Figure S8a (Supporting Information). The DRCN5T:STPH based NF-ASM OSCs also exhibited high device parameters with V_{oc} of 1.01 V, J_{sc} of 11.16 mA cm^{-2}, FF of 0.50, and PCE of 5.60% as shown in Table S6 (Supporting Information), approaching to the PCE of STPH based polymer solar cells using PTB7-Th as polymeric donor.[55] According to the absorption, the marginal difference of PCE between DRCN5T:STPH and DRCN5T:TPH is caused by the absorption ability in the range of 350–460 nm as shown in Figure S8b (Supporting Information). Since the frontier orbitals of TPH is strongly delocalized over the entire molecule, while those of STPH is localized on only one or two of the three PDI propellers. Thus the TPH acceptor has a stronger absorption ability than STPH as illustrated in previous literature.[79] These results demonstrate that the PDI derivatives can also be used as the electron acceptors to fabricate NF-ASM OSCs with higher PCEs.

In conclusion, we adopted a PDI derivative with 3D rylene architecture as electron acceptor and systematically investigated the effect of TA treatment on the BHJ morphology, molecular packing and orientation in the BHJ active layers. These results reveal that the acceptor molecules TPH have a greate influence on the molecular packing of donor DRCN5T that will weaken the crystalline in both in-plane and out-of-plane directions as well as the π–π stacking interaction in out-of-plane direction, making the DRCN5T molecules have a dominant face-on orientation in the BHJ active layer with TA treatment. In addition, TA treatment has a significant influence on the BHJ morphology and facilitates the crystalline and enhances the π–π stacking interaction of donor DRCN5T significantly, improving the PCE of DRCN5T:TPH based OSCs from 0.47% to 6.16%, among the highest PCEs for non-fullerene all-small-molecules OSCs. Additionally, the devices also showed a high V_{oc} of 1.04 V and a small E_{loss} of 0.56 eV, both parameters among best values for NF-ASM OSCs and even for polymer solar cells. As a result, the non-fullerene all-small-molecules OSCs are also good candidates for promoting the development of OSCs.

Supporting Information

Supporting Information is available from the Wiley Online Library or from the author.

Acknowledgements

The authors acknowledge the support from the National Natural Science Foundation of China (NSFC) (21225209, 91427303, 91333204, 21428304, 21504006, 21534003), the 973 Program (2014CB643500), and the Chinese Academy of Sciences (XDB12010100). X-ray data were acquired at beamlines 7.3.3 and 11.0.1.2 at the Advanced Light Source, which was supported by the Director, Office of Science, Office of Basic Energy Sciences, of the U.S. Department of Energy under Contract No. DE-AC02-05CH11231.

Received: July 29, 2016
Revised: September 27, 2016
Published online:

[1] G. Yu, J. Gao, J. C. Hummelen, F. Wudl, A. Heeger, *Science* **1995**, *270*, 1789.
[2] J. Chen, Y. Cao, *Acc. Chem. Res.* **2009**, *42*, 1709.
[3] Y. Li, *Acc. Chem. Res.* **2012**, *45*, 723.
[4] P. Beaujuge, J. Fréchet, *J. Am. Chem. Soc.* **2011**, *133*, 20009.
[5] Y. Liu, J. Zhao, Z. Li, C. Mu, W. Ma, H. Hu, K. Jiang, H. Lin, H. Ade, H. Yan, *Nat. Commun.* **2014**, *5*, 5293.
[6] L. Huo, T. Liu, X. Sun, Y. Cai, A. Heeger, Y. Sun, *Adv. Mater.* **2015**, *27*, 2938.
[7] H. Yao, W. Zhao, Z. Zheng, Y. Cui, J. Zhang, Z. Wei, J. Hou, *J. Mater. Chem., A* **2016**, *4*, 1708.
[8] W. Yue, R. Ashraf, C. Nielsen, E. Collado-Fregoso, M. Niazi, S. Yousaf, M. Kirkus, H. Chen, A. Amassian, J. Durrant, I. McCulloch, *Adv. Mater.* **2015**, *27*, 4702.
[9] Y. Hwang, H. Li, B. Courtright, S. Subramaniyan, S. Jenekhe, *Adv. Mater.* **2016**, *28*, 124.
[10] Y. Zhong, M. Trinh, R. Chen, G. Purdum, P. Khlyabich, M. Sezen, S. Oh, H. Zhu, B. Fowler, B. Zhang, W. Wang, C. Nam, M. Sfeir, C. Black, M. Steigerwald, Y. Loo, F. Ng, X. Zhu, C. Nuckolls, *Nat. Commun.* **2015**, *6*, 8242.
[11] D. Meng, D. Sun, C. Zhong, T. Liu, B. Fan, L. Huo, Y. Li, W. Jiang, H. Choi, T. Kim, J. Y. Kim, Y. Sun, Z. Wang, A. J. Heeger, *J. Am. Chem. Soc.* **2016**, *138*, 375.
[12] Y. Liu, L. Zhang, H. Lee, H. Wang, A. Santala, F. Liu, Y. Diao, A. Briseno, T. Russell, *Adv. Energy Mater.* **2015**, *5*, 1500195.
[13] K. Deshmukh, T. Qin, J. Gallaher, A. Liu, E. Gann, K. O'Donnell, L. Thomsen, J. Hodgkiss, S. Watkins, C. McNeill, *Energy Environ. Sci.* **2015**, *8*, 332.
[14] T. Earmme, Y. Hwang, S. Subramaniyan, S. Jenekhe, *Adv. Mater.* **2014**, *26*, 6080.
[15] J. Jung, J. Jo, C. Chueh, F. Liu, W. Jo, T. Russell, A. Jen, *Adv. Mater.* **2015**, *27*, 3310.
[16] C. Lee, H. Kang, W. Lee, T. Kim, K. Kim, H. Woo, C. Wang, B. Kim, *Adv. Mater.* **2015**, *27*, 2466.
[17] O. Kwon, M. Uddin, J. Park, S. Park, T. Nguyen, H. Woo, S. Park, *Adv. Mater.* **2016**, *28*, 910.
[18] H. Li, T. Earmme, S. Subramaniyan, S. Jenekhe, *Adv. Energy Mater.* **2015**, *5*, 1402041.
[19] Y. Wu, H. Bai, Z. Wang, P. Cheng, S. Zhu, Y. Wang, W. Ma, X. Zhan, *Energy Environ. Sci.* **2015**, *8*, 3215.
[20] Y. Li, X. Liu, F. Wu, Y. Zhou, Z. Jiang, B. Song, Y. Xia, Z. Zhang, F. Gao, O. Inganas, Y. Li, L. Liao, *J. Mater. Chem., A* **2016**, *4*, 5890.
[21] Y. Lin, Z. Zhang, H. Bai, J. Wang, Y. Yao, Y. Li, D. Zhu, X. Zhan, *Energy Environ. Sci.* **2015**, *8*, 610.
[22] W. Zhao, D. Qian, S. Zhang, S. Li, O Ingana, F. Gao, J. Hou, *Adv. Mater.* **2016**, *28*, 4734.
[23] Y. Li, L. Zhong, F. Wu, Y. Yuan, H. Bin, Z. Jiang, Z. Zhang, Z. Zhang, Y. Li, L. Liao, *Energy Environ. Sci.* **2016**, *9*, 3429.
[24] L. Gao, Z. Zhang, H. Bin, L. Xue, Y. Yang, C. Wang, F. Liu, T. Russell, Y. Li, *Adv. Mater.* **2016**, *28*, 8288.

[25] Y. Lin, F. Zhao, Q. He, L. Huo, Y. Wu, T. C. Parker, W. Ma, Y. Sun, C. Wang, D. Zhu, A. J. Heeger, S. R. Marder, X. Zhan, *J. Am. Chem. Soc.* **2016**, *138*, 4955.
[26] Y. Lin, Q. He, F. Zhao, L. Huo, J. Mai, X. Lu, C. Su, T. Li, J. Wang, J. Zhu, Y. Sun, C. Wang, X. Zhan, *J. Am. Chem. Soc.* **2016**, *138*, 2973.
[27] Y. Patil, R. Misra, M. Keshtov, G. Sharma, *J. Phys. Chem. C* **2016**, *120*, 6324.
[28] P. Josse, C. Dalinot, Y. Jiang, S. Dabos-Seignon, J. Roncali, P. Blanchard, C. Cabanetos, *J. Mater. Chem., A* **2016**, *4*, 250.
[29] J. Jung, W. Jo, *Chem. Mater.* **2015**, *27*, 6038.
[30] H. Shi, W. Fu, M. Shi, J. Ling, H. Chen, *J. Mater. Chem., A* **2015**, *3*, 1902.
[31] S. Li, W. Liu, M. Shi, J. Mai, T. Lau, J. Wan, X. H. Lu, C. Li, H. Chen, *Energy Environ. Sci.* **2016**, *9*, 604.
[32] T. Earmme, Y. Hwang, S. Subramaniyan, S. Jenekhe, *Adv. Mater.* **2014**, *26*, 6080.
[33] Y. Hwang, T. Earmme, B. Courtright, F. Eberle, S. Jenekhe, *J. Am. Chem. Soc.* **2015**, *137*, 4424.
[34] C. Mu, P. Liu, W. Ma, K. Jiang, J. Zhao, K. Zhang, Z. Chen; Z. Wei, Y. Yi, J. Wang, S. Yang, F. Huang, A. Facchetti, H. Ade, H. Yan, *Adv. Mater.* **2014**, *26*, 7224.
[35] B. Kan, Q. Zhang, M. Li, X. Wan, W. Ni, G. Long, Y. Wang, X. Yang, H. Feng, Y. Chen, *J. Am. Chem. Soc.* **2014**, *136*, 15529.
[36] Q. Zhang, B. Kan, F. Liu, G. Long, X. Wan, X. Chen, Y. Zuo, W. Ni, H. Zhang, M. Li, Z. Hu, F. Huang, Y. Cao, Z. Liang, M. Zhang, T. Russell, Y. Chen, *Nat. Photonics* **2016**, *9*, 35.
[37] Y. Liu, Y. Yang, C. Chen, Q. Chen, L. Dou, Z. Hong, G. Li, Y. Yang, *Adv. Mater.* **2013**, *25*, 4657.
[38] J. Wang, K. Liu, J. Yan, Z. Wu, F. Liu, F. Xiao, Z. Chang, H. Wu, Y. Cao, T. Russell, *J. Am. Chem. Soc.* **2016**, *138*, 7687.
[39] H. Bai, Y. Wang, P. Cheng, Y. Li, D. Zhu, X. Zhan, *ACS Appl. Mater. Interfaces* **2014**, *6*, 8426.
[40] P. Cheng, X. Zhao, W. Zhou, J. Hou, Y. Li, X. Zhan, *Org. Electron.* **2014**, *15*, 2270.
[41] J. Sun, A. Hendsbee, A. Dobson, G. Welch, I. Hill, *Org. Electron.* **2016**, *35*, 151.
[42] Y. Chen, X. Zhang, C. Zhan, J. Yao, *Phys. Status Solidi A* **2015**, *212*, 1961.
[43] Z. He, B. Xiao, F. Liu, H. Wu, Y. Yang, S. Xiao, C. Wang, T. Russel, Y. Cao, *Nat. Photonics* **2015**, *9*, 174.
[44] J. Huang, C. Li, C. Chueh, S. Liu, J. Yu, A. Jen, *Adv. Energy Mater.* **2015**, *5*, 1500406.
[45] Y. Liu, J. Zhao, Z. Li, C. Mu, W. Ma, H. Hu, K. Jiang, H. Lin, H. Ade, H. Yan, *Nat. Commun.* **2014**, *5*, 5293.
[46] J. Huang, J. Carpenter, C. Li, J. Yu, H. Ade, A. Jen, *Adv. Mater.* **2016**, *28*, 967.
[47] S. Li, L. Ye, W. Zhao, S. Zhang, S. Mukherjee, H. Ade, J. Hou, *Adv. Mater.* **2016**, DOI: 10.1002/adma.201602776.
[48] B. Kan, M. Li, Q. Zhang, F. Liu, X. Wan, Y. Wang, W. Ni, G. Long, X. Yang, H. Feng, Y. Zuo, M. Zhang, F. Huang, Y. Cao, T. P. Russell, Y. Chen, *J. Am. Chem. Soc.* **2015**, *137*, 3886.
[49] L. Gao, Z. Zhang, L. Xue, J. Min, J. Zhang, Z. Wei, Y. Li, *Adv. Mater.* **2016**, *28*, 1884.
[50] J. Jung, T. Russell, W. Jo, *Chem. Mater.* **2015**, *27*, 4865.
[51] O. Kwon, J. Park, D. Kim, S. Park, S. Park, *Adv. Mater.* **2015**, *27*, 1951.
[52] A. Sharenko, D. Gehrig, F. Laquai, T. Nguyen, *Chem. Mater.* **2014**, *26*, 4109.
[53] J. Sun, A. Hendsbee, A. Dobson, G. Welch, I. Hill, *Org. Electron.* **2016**, *35*, 151.
[54] A. Sharenko, C. M. Proctor, T. van der Poll, Z. Henson, T. Nguyen, G. Bazan, *Adv. Mater.* **2013**, *25*, 4403.
[55] J. Mikroyannidis, P. Suresh, G. Sharma, *Synth. Met.* **2010**, *160*, 932.
[56] H. Fan, X. Zhu, *Sci. China: Chem.* **2015**, *58*, 922.
[57] C. Zhan, S. Zhang, J. Yao, *RSC Adv.* **2015**, *5*, 93002.
[58] C. Zhan, J. Yao, *Chem. Mater.* **2016**, *28*, 1948.
[59] Z. Chen, A. Lohr, C. Saha-Moller, F. Wurthner, *Chem. Soc. Rev.* **2009**, *38*, 564.
[60] C. Li, H. Wonneberger, *Adv. Mater.* **2012**, *24*, 613.
[61] J. Liu, S. Chen, D. Qian, B. Gautam, G. Yang, J. Zhao, J. Bergqvist, F. Zhang, W. Ma, H. Ade, O. Inganas, K. Gundogdu, F. Gao, H. Yan, *Nat. Energy* **2016**, *1*, 16089.
[62] D. Meng, H. Fu, C. Xiao, X. Meng, T. Winands, W. Ma, W. Wei, B. Fan, L. Huo, N. Doltsinis, Y. Li, Y. Sun, Z. Wang, *J. Am. Chem. Soc.* **2016**, *138*, 10184.
[63] W. Jiang, L. Ye, X. Li, C. Xiao, F. Tan, W. Zhao, J. Hou, Z. Wang, *Chem. Commun.* **2014**, *50*, 1024.
[64] S. Rajaram, R. Shivanna, S. Kandappa, K. Narayan, *J. Phys. Chem. Lett.* **2012**, *3*, 2405.
[65] L. Ye, K. Sun, W. Jiang, S. Zhang, W. Zhao, H. Yao, Z. Wang, J. Hou, *ACS Appl. Mater. Interfaces* **2015**, *7*, 9274.
[66] N. Liang, K. Sun, Z. Zheng, H. Yao, G. Gao, X. Meng, Z. Wang, W. Ma, J. Hou, *Adv. Energy Mater.* **2016**, *6*, 1600060.
[67] Q. Wu, D. Zhao, A. Schneider, W. Chen, L. Yu, *J. Am. Chem. Soc.* **2016**, *138*, 7248.
[68] J. Lee, R. Singh, D. Sin, H. Kim, K. Song, K. Cho, *Adv. Mater.* **2016**, *28*, 69.
[69] Y. Lin, Y. Wang, J. Wang, J. Hou, Y. Li, D. Zhu, X. Zhan, *Adv. Mater.* **2014**, *26*, 5137.
[70] Y. Liu, C. Mu, K. Jiang, J. Zhao, Y. Li, L. Zhang, Z. Li, J. Lai, H. Hu, T. Ma, R. Hu, D. Yu, X. Huang, B. Tang, H. Yan, *Adv. Mater.* **2015**, *27*, 1015.
[71] B. Jing, Y. Li., H. Lin, Y. Liu, K. Jiang, C. Mu, T. Ma, J. Lai, H. Hu, D. Yu, H. Yan, *Energy Environ. Sci.* **2015**, *8*, 520.
[72] W. Li, K. Hendriks, A. Furlan, M. Wienk, R. Janssen, *J. Am. Chem. Soc.* **2015**, *137*, 2231.
[73] K. Vandewal, A. Gadisa, W. D. Oosterbaan, S. Bertho, F. Banishoeib, I. Van Severen, L. Lutsen, T. Cleij, D. Vanderzande, J. Manca, *Adv. Funct. Mater.* **2008**, *18*, 2064.
[74] M. Wang, H. Wang, T. Yokoyama, X. Liu, Y. Huang, Y. Zhang, T. Q. Nguyen, S. Aramaki, G. C. Bazan, *J. Am. Chem. Soc.* **2014**, *136*, 12576.
[75] D. Veldman, S. C. J. Meskers, R. Janssen, *Adv. Funct. Mater.* **2009**, *19*, 1939.
[76] K. Kawashima, Y. Tamai, H. Ohkita, I. Osaka, K. Takimiya, *Nat. Commun.* **2015**, *6*, 10085.
[77] E. Gann, A. Young, B. Collins, H. Yan, J. Nasiatka, H. Padmore, H. Ade, A. Hexemer, C. Wang, *Rev. Sci. Instrum.* **2012**, *83*, 045110.
[78] A. Hexemer, W. Bras, J. Glossinger, E. Schaible, E. Gann, R. Kirian, A. MacDowell, M. Church, B. Rude, H. Padmore, *J. Phys. Conf. Ser.* **2010**, *247*, 012007.
[79] S. Li, W. Liu, C. Li, F. Liu, Y. Zhang, M. Shi, H. Chen, T. Russell, *J. Mater. Chem., A* **2016**, *4*, 10659.